Updated Conceptual Model and Reserve Estimate for the Salton Sea Geothermal Field, Imperial Valley, California

Dennis Kaspereit[1], Mary Mann[1], Subir Sanyal[1], Bill Rickard[1], William Osborn[1], and Jeff Hulen[2]

[1]Geothermal Resource Group, Palm Desert CA
[2]Private Consultant, Ivins UT
dkaspereit@geothermalresourcegroup.com • mary@geothermalresourcegroup.com
ssanyal@geothermalresourcegroup.com • billrickard@geothermalresourcegroup.com
wosborn@geothermalresourcegroup.com • jbh_rmh@kayenta.net

Keywords
Salton Sea, reserves, potential, pull-apart, conceptual model, heat anomaly, rift, magnetotelluric, seismic

ABSTRACT

The Salton Sea Geothermal Field is one of the largest geothermal resources in the world. Recent changes in leasehold positions, changes in lake management due to Colorado River water transfers, a transition to renewable energy resources and the clean energy initiatives of California, have prompted renewed interest in development of the field for baseload power generation. The receding shoreline of the Salton Sea is now exposing areas previously inaccessible, and exposing large tracts of land for development.

Since the last conceptual model and resource estimate for the Salton Sea Geothermal Field was published in 2002, significant additional data has become available, including publicly available seismic surveys over the resource area, experiences of developers and operators at the field, and recent research related to seismicity and tectonics of Southern California. In this study, we integrate these data sets in an updated conceptual model and a revised estimate of the power generation potential of the field. The result is a model that can serve as the basis for further exploration and development in the field. Our study increases the power generation potential of the field to 2950 MW_e.

Introduction

The Salton Sea Geothermal Field (SSGF) has been explored since 1927, and in commercial production since 1982. Our understanding of the field has increased considerably over that time. This paper is an update of the conceptual model and reserve estimate originally presented in *Refined Conceptual Model and a New Reserve Estimate for the Salton Sea Geothermal Field, Imperial Valley, California* (Hulen et al., 2002), which presented a conceptual model of the entire SSGF. Hulen et al. (2002) refined the previous conceptual model based on extensive drilling data from the land portion of the field, combined with shallow temperature gradient drill hole measurements. No new data points were available from the submerged part of the SSGF, making the refinement and estimates less detailed in that part of the field. It is widely believed that significant potential exists in the submerged portion of the lake, likely more potential than on dry land.

The Salton Sea has been receding, and is expected to recede faster after 2017 due to implementation of a 2003 water transfer agreement. The receding lake has opened up significant lands, formally submerged and unavailable to geothermal development. At least one project has been announced on the former lake bed, and the newly exposed areas of the SSGF are expected to be a central part of future geothermal development.

The SSGF is a robust world class geothermal field, primarily because of its structural setting. The SSGF is located in the Salton Trough, a tectonically active sedimentary pull-apart basin that occurs at the southern tip of the San Andreas fault system as it steps over into the continental rift zone between the Pacific and North American Plates. The Salton Trough, south into the Gulf of California, is dominated by a series of smaller scale pull-apart basins of different sizes that connect right-stepping, primarily right-lateral, strike-slip faults that strike generally northwest (Figure 1). This pattern of

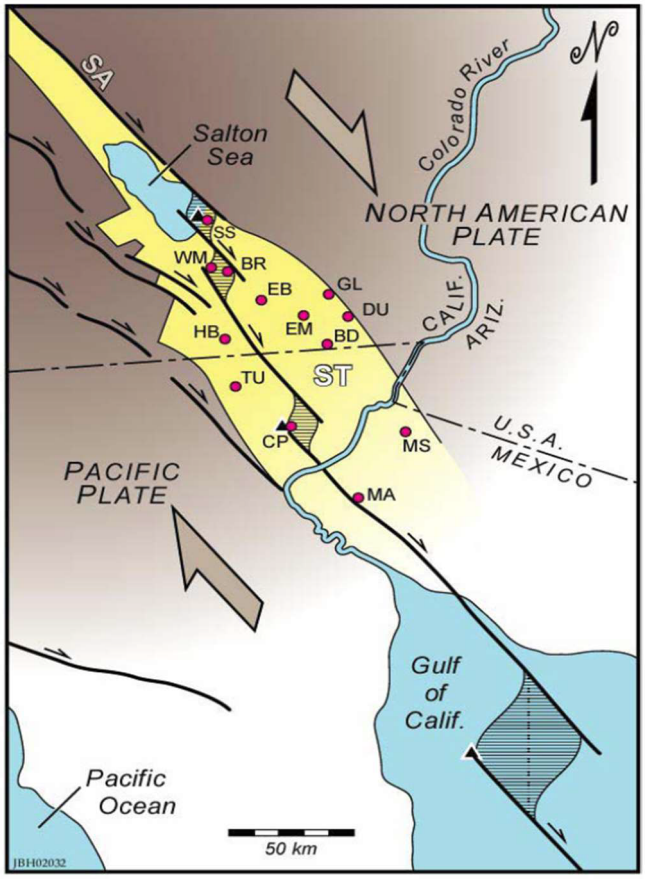

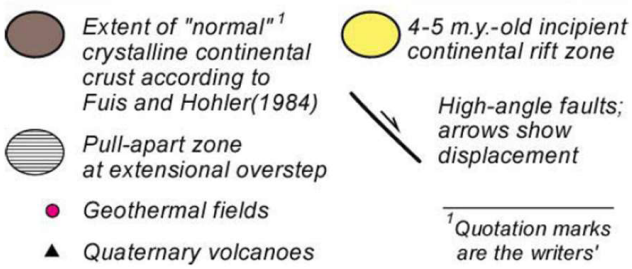

Figure 1. Location and tectonic map of the Salton Trough (ST) and its high temperature geothermal systems relative to the southeastern terminus of the San Andreas fault zone (SA) and the tip of the Gulf of California. Geothermal fields (not all currently producing) are abbreviated and shown with red dots. Large arrows show modern relative motion of tectonic plates. Note location of Salton Sea (SS) and Cerro Prieto (CP) geothermal fields within two prominent pull-apart zones, which also host the Trough's exposed Quaternary volcanoes. Synthesized and re-drawn from Elders et al. (1982), Lachenbruch et al. (1985), and Elders and Sass (1988), from Hulen et al. (2002).

faulting forms in transtensional shear zones where there are structures related to both strike-slip and extension.

Tectonically, the formation of the SSGF is influenced not only by the step-over from the San Andreas fault (SAF) to the Imperial fault (IF), but also by the San Jacinto fault zone (SJFZ) which runs up the west side of the Salton Sea, which joins the SAF to the north. This impedes the northern movement of the Pacific Plate between the SAF and SJFZ zone, transferring most of the northern motion west of the SJFZ. This imparts rotation of a larger land area and increases the complexity, forming two spreading centers within the larger step-over (Figure 2) (Brothers et al., 2009). The Brothers et al. tectonic model highlights two spreading and expansion centers, or extensional domains (shown as blue boxes in Figure 2c), within the larger step-over from the San Andreas fault to the Imperial fault, with each center containing a geothermal field. The pull-apart extension is primarily accommodated along duplex R' Riedel shear faults within the larger tectonic regime. The extension creates crustal thinning, and facilitates igneous intrusion and volcanism, and the

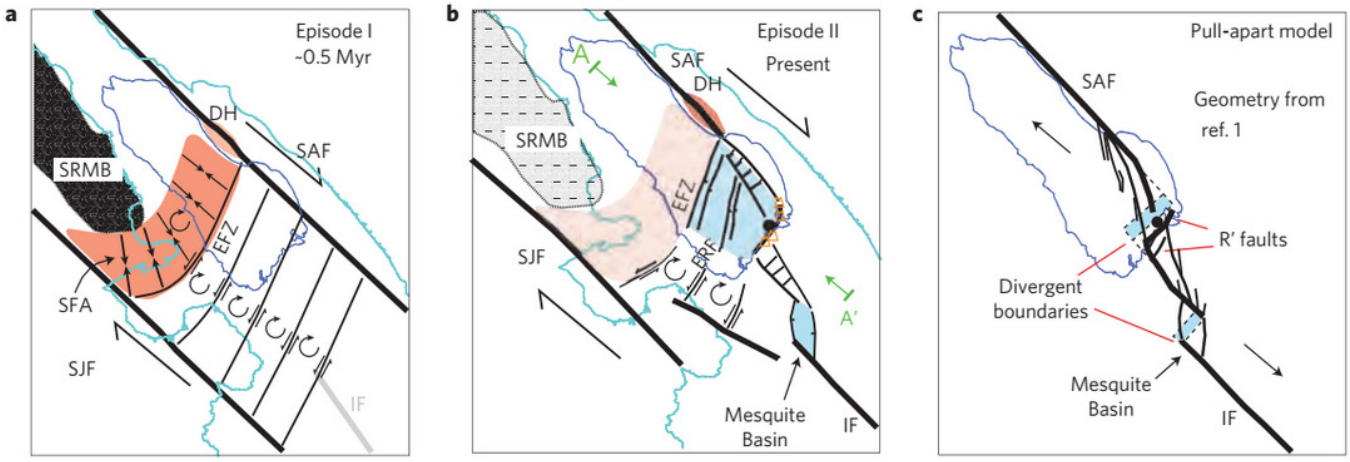

Figure 2. Map-view models of the tectonic evolution of the Salton Sea. a. Block rotation between the San Andreas Fault (SAF) and the San Jacinto Fault (SJF) and compression north of Extra fault zone (EFZ) at ~.5 Myr b. Development of SAF-Imperial Fault (IF) step-over and present-day configuration. c. Physical model of a pull-apart basin with mechanical layering (superimposed on the Salton Sea). Bold black lines represent the primary tectonic structure, orange triangles are volcanic buttes, blue shades in b and c are extensional domains, light-red zones in a and b are inactive compression, dark-red zones in a and b are active compression, blue line in a and b is the ancient lake Cahuilla shoreline, green arrows labeled A-A' in b define the extent of the cross section view in Figure 13. Extension is focused along R' faults above the divergent boundary. The lower blue box (2c) is the Mesquite Basin, where the Brawley field is located, and represents a separate pull-apart basin within the SAF-IF step-over. The other, upper blue box is the Salton Sea basin in which the SSGF is located (Brothers, 2009).

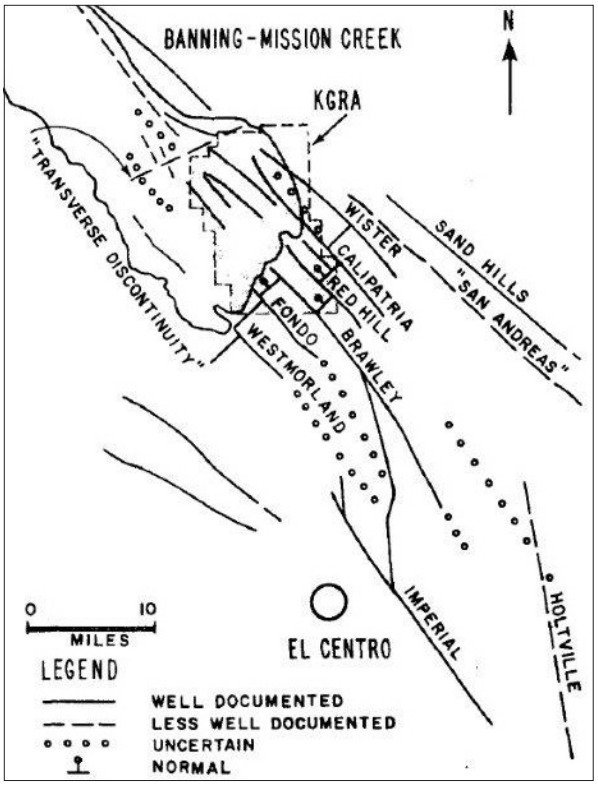

Figure 3. Structural map of the Salton Sea Geothermal Field (SSGF) based on combined geophysical data originally published in Meidav and Howard (1979).

with oblique slip, i.e. hybrids of strike-slip and normal-slip faults, with extension still being the major component. The faults in this map terminate at the edge of the lake, as they were not able to be mapped in the areas that were submerged at the time.

Recorded and relocated seismicity shows evidence of the faulting continuing into the lake (Figure 4). In addition to showing the activity of the faults described previously, Figure 4 also shows that the seismicity around the SSGF has distinct eastern and western seismic clusters. Faults in the western cluster are aligned at a different angle than the eastern cluster. This is consistent with the tectonics mentioned and shown in Figure 2. In Figure 4, plate motion is shown outside of the SAF and SJFZ (large half arrows), with an insert showing the connection of the two faults to the north. This impedes the northern movement between the SAF and SJFZ and results in rotation within in the field, changing some fault orientations within the field. The rotation is centered at the end of the SJFZ and at the western end of the Elmore Ranch fault which is oriented east-northeast across the southern end of the Salton Sea to the northwestern side of the SSGF. Seismicity stops north of the Elmore Ranch fault within the SSGF, which could indicate that this is the northern boundary for the western side (cluster) of the SSGF, consistent with the boundary by other methods to be presented below. There is frequent seismic activity within the current production areas of the SSGF.

dramatically elevated heat flux that supports the region's high grade geothermal systems. The northern extension domain (blue box) in Figure 2c is the SSGF.

These tectonic influences have created a complex system involving several unusual observations, including the peculiar pork chop shape of the field, one side of the field rising while the other is subsiding, the different orientation of the Brawley fault, stepping fault lines, geochemical inconsistencies, areas of distinct geologic disturbances, and the formation of rhyolite domes in a unique pattern. Until now, no conceptual model of the SSGF has incorporated and resolved these observations into a single model.

Overview of Faults and Structure

Several faults are mapped within the larger Salton Trough, as shown in Figure 3 (Meidav and Howard, 1979). The faults were detected using geophysical methods and have been further confirmed with field observation and additional geophysical surveys (Lynch and Hudnut, 2008). North-dipping normal faults were interpreted perpendicular to the main northwest striking faults, as would be predicted for the bounding faults of an extensional tectonic regime. These faults are now interpreted to be R' Riedel shear faults that have evolved as part of a duplex strike-slip regime

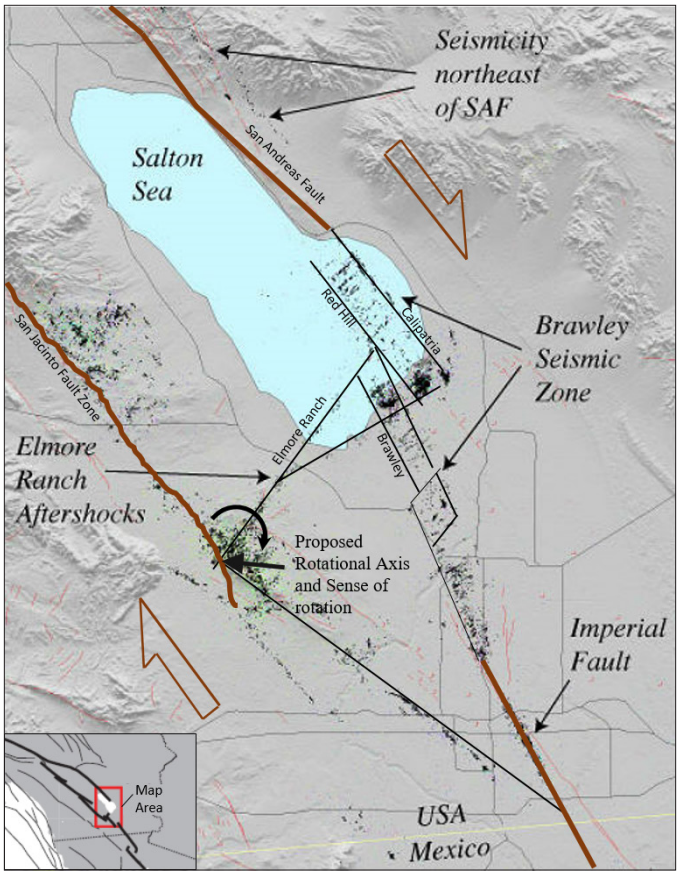

Figure 4. Salton Trough seismicity, with colored dots show recorded seismic events from 1981 to 2005. They cluster to form distinct patterns that reveal the fault-bounded block rotation at the southern end of the Salton Sea. Modified from Shearer et al. (2005). Insert from Brothers et al. (2009).

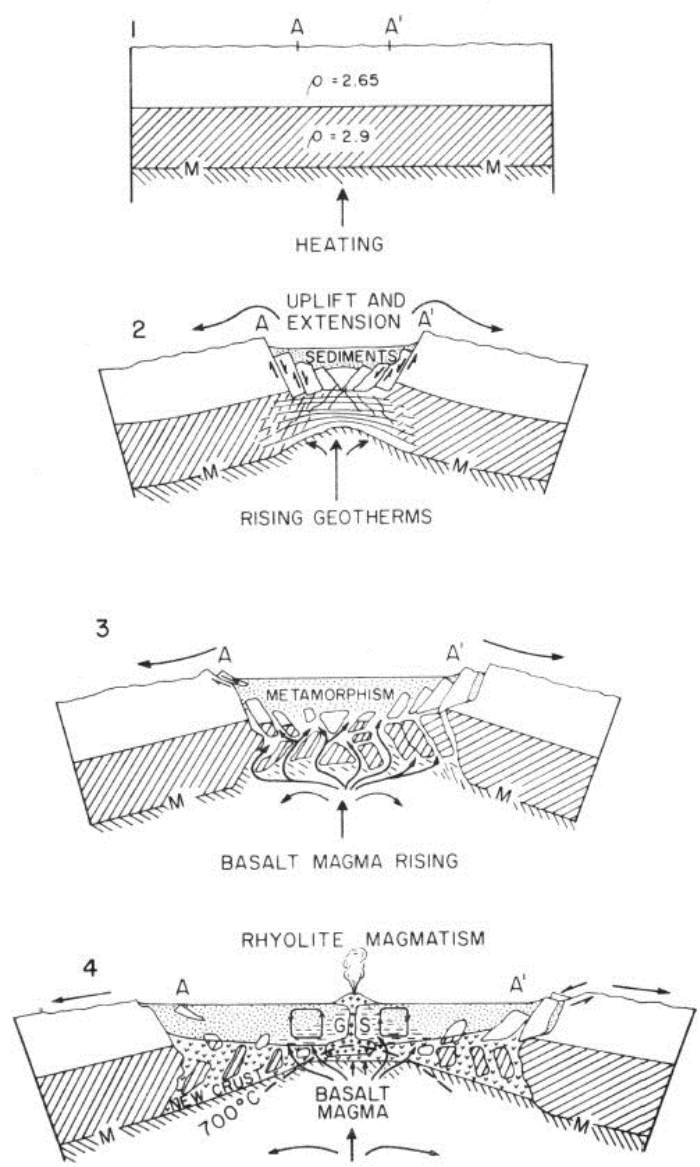

Figure 5. Model of pull-apart extension and magma extrusion. Stage 1: two layers of crust overlie a hot zone in the mantle. M, Moho discontinuity; A and A' reference points for later movements. Stage 2: Upward and lateral expansion - a trough is initiated and partly filled by sediments. Stage 3: The widening trough is invaded by basaltic magma - metamorphism of the sediments and gravitational sliding of the tilted walls occurs. Stage 4: Melting of the basement and extrusion of rhyolitic magma - ascending hot brine causes greenschist metamorphism (GS) at shallow depth (Elders, 1979).

It is apparent that the SSGF does not occupy a simple pull-apart basin and structure, but rather one significantly modified by much larger scale crustal-block rotation.

Formation of Extension Zones

This reserve estimate uses a simplified transtensional pull-apart model to approximate the location of the hottest and most productive parts of the SSGF system, as well as the system's lateral extent. This model explains many of the characteristics of the SSGF.

In a purely extensional model, pull-apart basins form as a result of symmetric extensional forces that pull the crust apart (Figure 5). The center of the pull-apart zone, where the crust is the thinnest, is where the rhyolite domes are most likely to break the surface, such as we have in the SSGF. Fracturing should be fairly equal on either side of the centerline.

Applying the extensional concept to the Salton Trough and SSGF field, each volcanic center can be envisioned as being localized at the center of an individual pull-apart zone within the larger pull-apart basin (Figure 6-4). In Figure 6b a red line is drawn in the center, over the rhyolite dome in each separate zone. The yellow lines mark the outer boundaries of the extensional fracturing in each separate pull-apart zone. The open faults (seismicity clusters in Figure 4) run parallel to these boundaries which are nearly perpendicular to the strike-slip faults. Faulting is expected to be more prevalent, and the thermal gradient higher, as the centerline of each extension zone is approached. In the case of the Salton Sea basin, sedimentation is more prevalent and the thinning exaggerated within the sub-pull-apart zones, but the general model illustrates the concept that the individual zones of extension provide permeability for magma intrusion

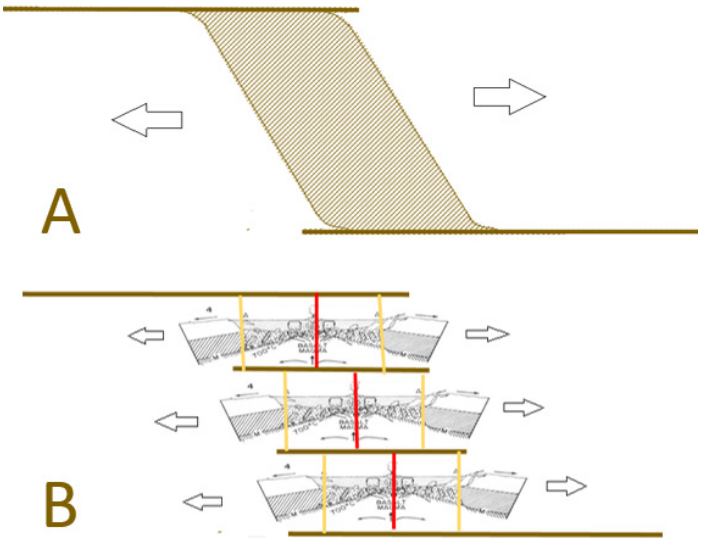

Figure 6. A) A highly simplified conceptual pull-apart basin on a regional scale in plan view. B) Same spreading center basin showing the concept for smaller scale pull-apart zones within the larger basin. The lines are in plan view and the sections should be envisioned in cross-sectional view. The red line is in the center of the pull-apart zone, which is typically the thinnest and most likely place for surface thermal features to form, and have the most faulting. The yellow line marks the outer boundary of the pull-apart zone and shows symmetry around the spreading basin between strike-slip faults.

and thermal fluid convection within the larger pull-apart basin.

Figure 7 shows a proposed structure map of the SSGF using a symmetric transtensional-extension model, using the same colored centerline and extension boundaries as in Figure 6b (shown orientated in insert). The proposed structures are projected over the shallow thermal gradient anomaly that was presented in the previous conceptual model of Hulen et al. (2002). The three thicker, brown lines represent the northwest-trending, en echelon, dextral strike-slip faults named, from east to west, Calipatria, Red Hill, and Brawley. These faults are envisioned as the major faults in the field. The thinner lines between those faults represent the minor faults and have been identified by well intersections and surface features. The Red Hill fault has an apparent vertical component of slip. The area between the Red Hill fault and the Calipatria fault is rising relative to the area southwest of the Red Hill fault from subsidence surveys. There is also a difference in brine properties across the Red Hill fault. The subsidence may be associated with the change in orientation—the twist and separation—of the northwest striking faults southwest of the Red Hill fault.

The five SW-NE red line segments (Figure 7) perpendicular to the main faults represent the hypothetical centerlines of the pull-apart zones between each set of the strike-slip faults based on the presence of the rhyolite domes at these locations. These domes can be assumed to have been intruded at the weakest points in the crust, where magma came to the surface in the recent past. The southeastern boundaries of the field are marked by the southern yellow lines. These boundaries have been confirmed and adjusted based on drilling results. The pattern of seismic activity also reveals the edges of the SSGF where the seismic activity diminishes. The placement of the brown line segments, also perpendicular to the main faults, is based on the presence of shallow thermal features that are believed to be indicators of active faults. The boundaries on the southeastern side have been mirrored on the northwest side of the field, presuming symmetry.

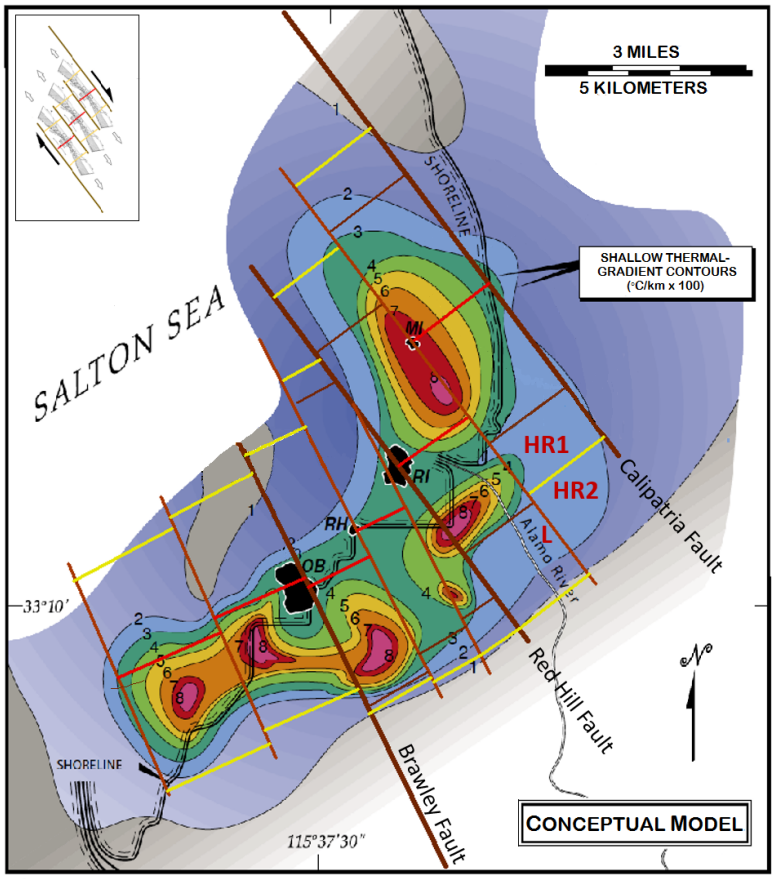

Figure 7. Interpreted SSGF pull-apart extension structure imposed on the shallow thermal gradient map of Hulen et al (2002). Thick brown northwest striking faults are documented in literature, thinner brown faults have been identified in well cuttings and conceptualized. Perpendicular red lines are the conceptual pull-apart centers, the yellow lines represent the extent of the extensional systems. The shallow thermal gradient anomaly is based on data available through June 2002, revised and updated from Newmark et al. (1988). MI–Mullet Island; OB–Obsidian Butte; RH–Rock Hill; RI–Red Island; HR1-Hudson Ranch 1; HR2-Hudson Ranch 2, L-Leathers.

Regional Influence

For targeting of wells for resource development, the exact orientation and location of the currently active strike-slip and extensional structures should be confirmed with further geophysical work The faulting and fracturing associated with the pull-apart zones may not be regular or perpendicular, but the assumption is

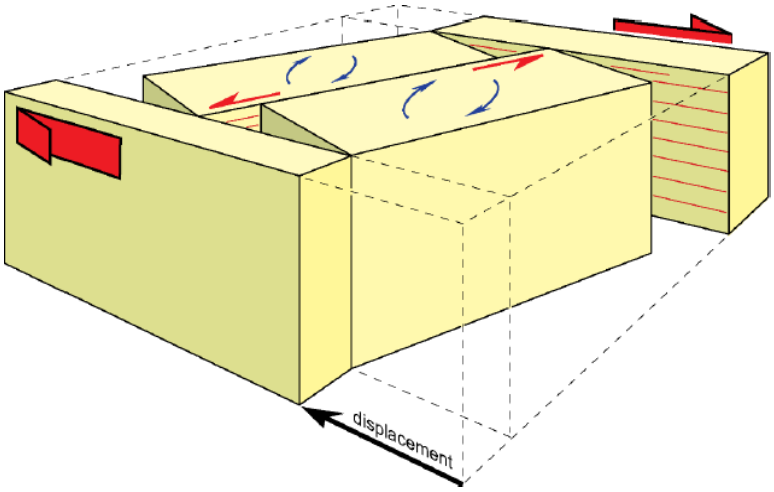

Figure 8. Besides the major expansion component, fault blocks between the major strike-slip faults would also have a small component of left lateral slip shown by the smaller red arrows, and some rotation shown by the blue arrows. Slip and rotation motion is exaggerated (Burg, 1986).

acceptable for resource estimation. Extensional forces are the primary control on the location of the most active parts of geothermal field. This is illustrated by the seismic activity that forms a ladder-like pattern (Figure 4) revealing the extensional faults.

As alluded to previously, due to the regional tectonic regime (Figures 2 and 4) the faulted blocks of the SSGF system have a component of rotation, which is conceptualized in Figure 8. The rotation may create openings at the tips or intersections of the faults, which could be especially permeable drilling targets, particularly where this is more apparent on the western side of the SSGF.

Shallow Heat Anomaly

The original shallow heat anomaly map of the SSGF was generated using data from drilling programs conducted in 1982 and 1985, and some onshore data from early wells (Newmark et al., 1988). Newmark et al. showed that the SSGF extended beneath the lake along with two high thermal gradient areas, both offshore, one to the southwest of the power plants previously operated by Unocal, and another to the northeast, offshore of Red Hill and running northwest and beyond Mullet Island.

With additional drilling onshore, a revised map was compiled in 2002 (Figures 7 and 9). This map included high thermal gradient areas onshore over the western Unocal power plant area and southeast of Obsidian Butte, and another southeast of the bay at Red Hill. The Imperial and Hudson Ranch areas to the east, also proved to be productive based on drilling results, as did the Leathers area to the southeast, as shown in Figure 9 (between the 1988 contour (orange) and 2002 contour (black-dashed)). Although the extent of the thermal anomaly onshore increased significantly with the additional data, the offshore portion was largely unchanged as the only additional data was the drilling of IID-14 on Red Hill. IID-14 demonstrated that the shallow heat anomaly edge may not be correct at this location. The well is on the edge of the shallow gradient anomaly, although it is the hottest well in the field at 390˚C (734˚F) at reservoir depths. Thus, the shallow heat anomaly does not accurately define the boundary of the deeper geothermal reservoir and, instead, should be used only to broadly define the field margins. Further exploration should proceed with geophysical surveys designed to reveal information about the deeper subsurface.

No targeted geophysical surveys were conducted within the SSGF before the last publicly available field wide assessment was completed in 2002. Since then, an onshore and offshore MT survey has been completed, as well as an onshore 3D seismic survey. With additional drilling completed since 2002, and the availability of other data, a better assessment can now be conducted.

A component missing in the contours of the shallow heat anomaly maps is the geophysical structure. Contouring previously was done using gradient data points only, with smooth contouring around them. Almost all of the 200°C/km contour of the shallow heat anomaly can be re-contoured to the limits of the symmetric extension model while still honoring the shallow heat anomaly data points, as shown in Figure 9. An exception is in the western area where the green outline is drawn due to two anomalously low data points. These two exceptions will be addressed below in the discussion of seismicity. Using the proposed structure developed by the symmetric extension model in Figure 7, the 200°C/km contour of the shallow heat anomaly has been redrawn in red and

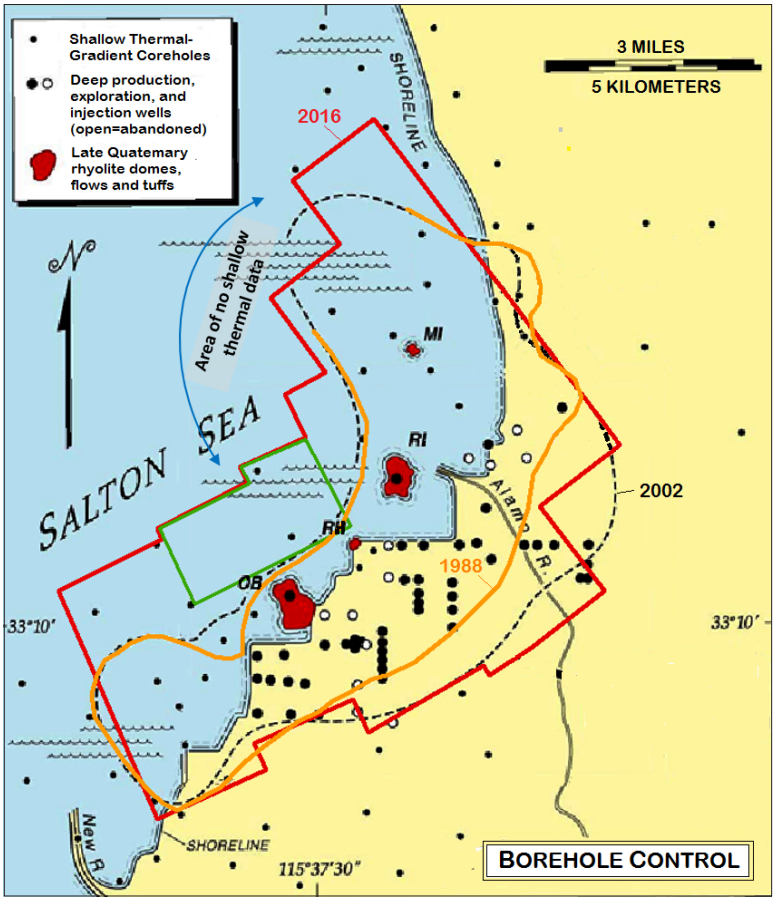

Figure 9. Borehole control for the shallow heat anomaly, with outline from Hulen (2002) in a dashed black line, and a re-contoured boundary (shown in red) using the symmetric extension model as a basis for boundaries. Green outline is where two shallow data points do not match the model. The original 1988 shallow heat anomaly boundary is shown in orange, open to the northwest. A data gap on the northwest edge of the shallow heat anomaly is noted by a blue arc.

shown in Figure 9. The original 1988 line, the 2002 line, and the new 2016 line are shown on the map in orange, black-dash, and red, respectively.

While the Hudson Ranch 1 (HR1) and Leathers (L) power plants were originally outside the limits of the shallow heat anomaly gradient limit, these two plants, as well as the Hudson Ranch 2 (HR2) development, are within the 2002 limit. From Figure 7, it is apparent that the unsuccessful HR2 project in the southeast corner of the field is outside the boundary of the symmetric extension model and, therefore, also outside of the limits of the 2016 shallow heat anomaly, providing validation to the extension model. The currently producing HR1 and Leathers plants are located in both the symmetric extension model and the 2002 shallow heat anomaly contour. It seems difficult to contour or otherwise explain the exclusion of HR2 without the symmetric extension model.

The shallow heat anomaly boundary is poorly constrained to the northwest, as there are no thermal gradient holes within the area indicated by the curved thin blue arc in Figure 9. However, there is geophysical evidence (regional magnetic and gravity data) that suggests the boundary of the SSGF in this area.

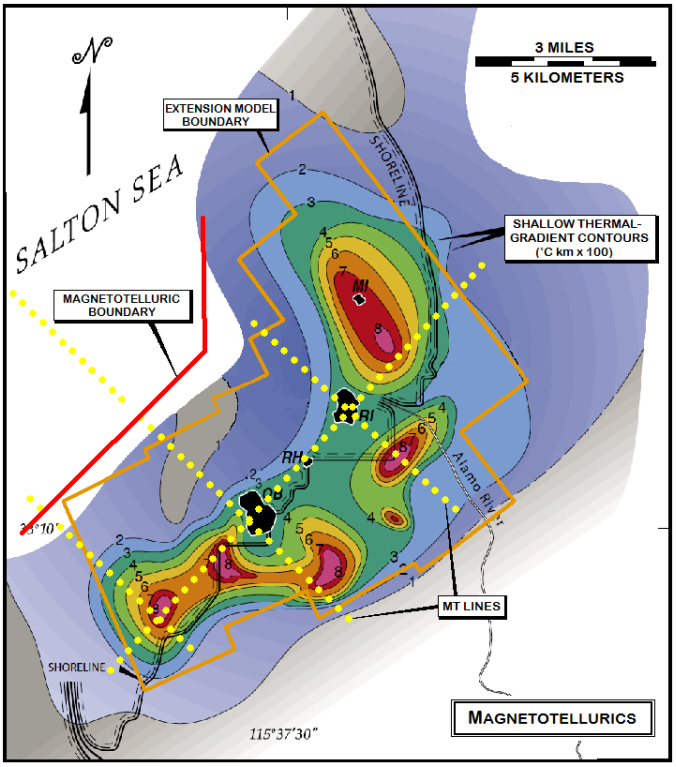

Figure 10. Yellow dotted lines show location of MT stations from 2003-2009 study, and red line approximates the boundary of the geothermal field as interpreted study, and the orange border is the field boundary from the current conceptual model. (Modified base map is from Hulen et al. 2002, and reprinted in Schlumberger, 2009).

Magnetotellurics

While geophysical data was difficult to obtain over much of the SSGF while it was submerged, a research project was conducted from 2003 to 2009 to pioneer the use of offshore magnetotellurics (MT) (Kaspereit et al., 2006; Nichols, 2009). The project was primarily to improve oil and gas exploration techniques, but was done at the SSGF because the Salton Sea allowed a research environment with calm water, and a unique opportunity of allowing comparison between adjacent onshore and offshore MT survey areas. The survey provided publicly available MT data in the submerged areas of SSGF. The dotted lines superimposed on the thermal gradient map in Figure 10 show the MT survey lines, with half onshore, half offshore, and a tie line down the shoreline.

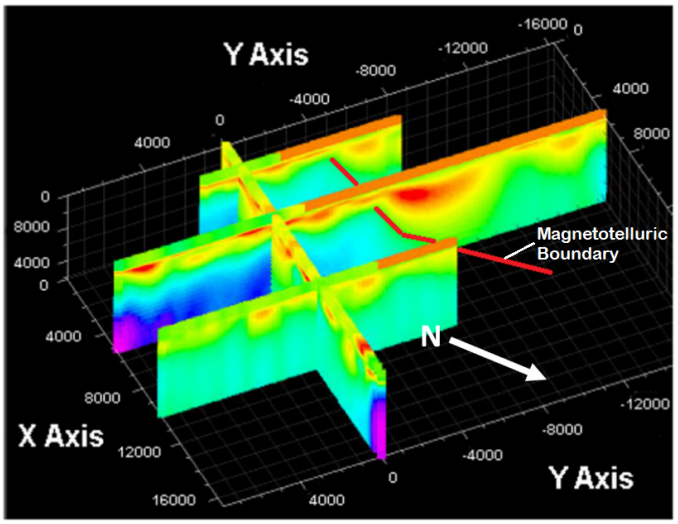

Figure 11. Three dimensional visualization of the subsurface electrical resistivity distribution of four survey profile lines, with the red line showing approximate location of northwest boundary of the geothermal field as interpreted from study (after Schlumberger, 2009). Resistivity is higher in the blue spectrum and more conductive toward red.

A 3D interpretation of the MT resistivity reveals the offshore boundary of the field (Figure 11). The offshore boundary is the edge where the resistive basement appears to be deeper and the less resistive sediments are the thickest. The intrusive basement thought to be the heat source for the SSGF would have a more resistive signature (blue/green) than the sediments of the Salton Sea basin (orange/red). The boundary is at least 4,000 meters (13,125 feet) northwest of the station line that runs southwest to northeast along the shoreline, and becomes farther from the shore traveling northeast along the shoreline stations, after passing the middle survey line. These limits are consistent with the symmetric extension model and the location that the model defines for the northwest boundary, although it conflicts with the shallow heat anomaly boundary in this area.

There is good agreement on the location of the northwest boundary from the MT data and the extension model (Figure 10), with the MT boundary representing the outer thermal boundary and the extension model representing the inside permeability boundary.

Seismic

An active seismic survey conducted in 2009 (Brothers et al., 2009) as part of the Salton Sea Imaging Project extends from the northern end of the Salton Sea to near the southern shore between Obsidian Butte and Rock Hill, the two southernmost rhyolite domes (Figure 12). A significant result of this survey was the identification of a 'gas phase', likely to be water vapor plus carbon dioxide in this case, which extends farther northwest of what has previously been interpreted as the edge of the geothermal field (Figure 13). This implies that the geothermal reservoir extends significantly in the northwest direction, although the extent is poorly constrained.

The interpreted gas or vapor phase boundary extends into the area where the shallow heat anomaly does not match the symmetric extension model (green area in Figure 9). The gas phase appears deeper to the northwest, in faulted steps, where there is no indication of a shallow gas phase (from the gradient wells). These faulted steps could explain the limited extent of the shallow heat anomaly in this area.

It also shows the formation becoming shallower approaching the "hinge zone" in Figure 13. The hinge zone occurs in the area north of which, the seismic activity is greatly reduced.

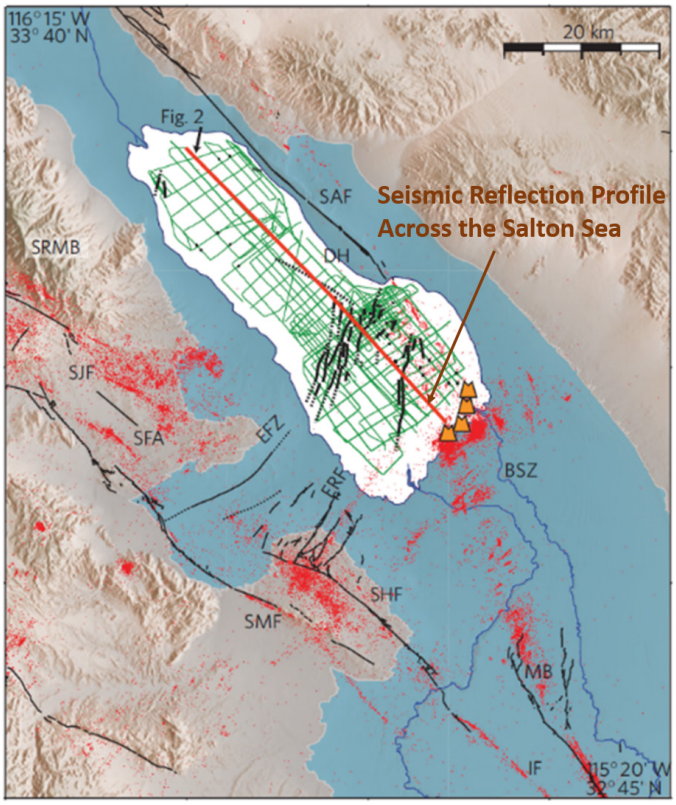

Figure 12. Location of seismic line across the Salton Sea shown in Figure13 (red line), recorded seismic events (red dots), mapped faults (black lines), and seismic reflection profiles (green lines) (Brothers et al., 2009).

Power Generation Potential of the SSGF

The Salton Sea is one of the world's most prolific resources as a result of high heat flow due to the field's tectonic setting, and the host sedimentary formations. The power generation potential of 2330 $MW_{e,}$ estimated by Hulen et al

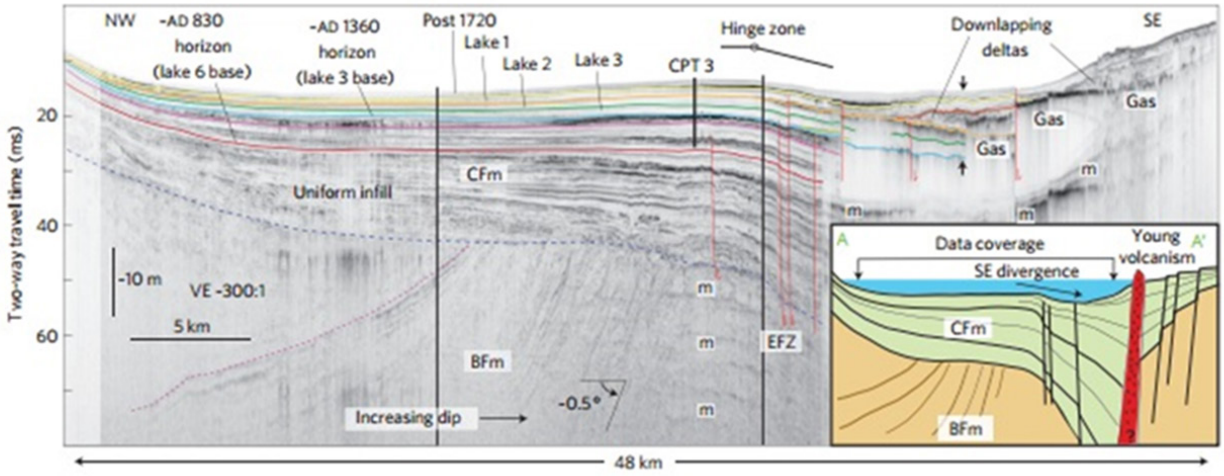

Salton Sea long-axis seismic reflection profile. A truncation surface (dashed blue line) separates the Holocene CFm from the underlying Pleistocene BFm. Coloured horizons represent time horizons in the CFm; red lines denote faults; black arrows mark the location at which sedimentation rate was estimated; multiple reflections (acoustic artefacts) are identified by 'm'. The black pipe labelled CPT-3 represents cone penetration test data (see Supplementary Fig. S1). Inset, Interpretive cross-section. North of the EFZ, reflectors in the CFm are concordant and record little deformation. Reflectors in the BFm show evidence for ~N/S-oriented compression. South of the EFZ, layers diverge and thicken. We infer that maximum subsidence occurs near the southern shoreline and that extensional faults may provide fluid migration pathways for young volcanism.

Figure 13. Salton Sea seismic reflection profile along survey line shown in Figure 12. The interpretation indicates that extensional faulting at the southern end of the seismic line provides the fluid pathways for young volcanism. Note gas effect is not as shallow at black arrows as is apparent closer to shore. Depth is exaggerated (Brothers et al., 2009).

(2002), established the SSGF as the largest geothermal field in the United States. That estimate was based on a thermal anomaly and available well data covering 72.4 km^2. Since 2002, extensive exploration, drilling, and denser and better data acquisition from the land portion of the field has expanded the limits of the anomaly. As exploration moves into the formally submerged part of the Salton Sea, where data is sparse, the actual field-boundary in that area is becoming clearer. As shown in this paper, like the land portion, the shallow heat anomaly does not fully define the limit of the geothermal resource.

Using a more refined model and structure within the field puts constraints on the anomaly where drilling data is not available, and a more accurate field boundary is achieved. The new field boundary (Figure 14) encompasses an area of 91.9 km^2. Using the same methodology as Hulen et al (2002) to calculate power potential yields a new estimate of 2,950 MW$_e$.

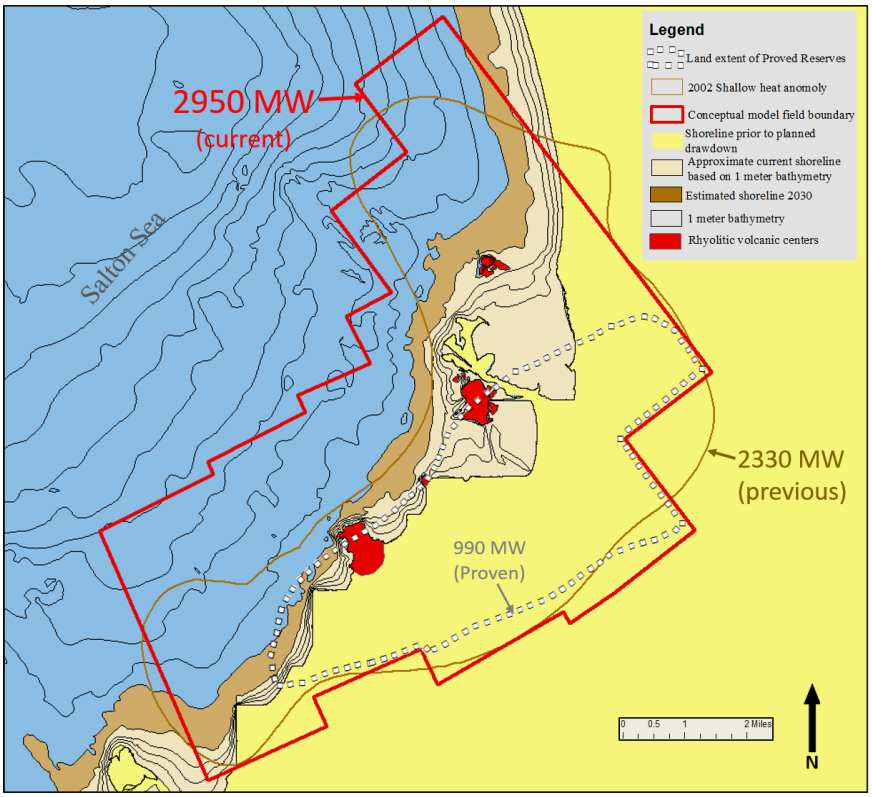

Figure 14. Outline of previous reservoir limit based on the shallow heat anomaly shown in brown, with the new boundary based on the new conceptual model shown in red. Proved reserves are shown by the dotted white outline. Light brown is the area, and reserves, that has been exposed by the receding sea to date, and the darker brown area is the additional area that will be exposed before a project could be completed. Directional drilling could extent the area by ½ mile from pads on the exposed lakebed.

Of the new estimated power potential, 1,130 MW$_e$ or 38% is on the previous dry land area. The receding lake has exposed an additional 545 MW$_e$ of potential probable, and proved reserves, and another 265 MW$_e$ of potential reserves will be exposed by the time any project development could be completed. Directional wells can reach farther horizontally (up to ½ mile) that could tap 310 MW$_e$ of potential possible reserves. Added together the former offshore area that is drillable by potential current projects is 1120 MW$_e$, almost the same amount on the previous dry land area. Together, 2,250 MW$_e$ is currently developable, with the remaining 700 MW$_e$ becoming increasing accessible by 2030.

Of the total 2,250 MW$_e$ currently developable, 990 MW$_e$ is proven, of which 392 MW$_e$ is on-line. Over one gigawatt of the remaining reserves are probable.

Conclusion

The newly exposed lake bed within the SSGF is the premier geothermal development area in the United States. The receding lake has exposed previous lake bed that alone has the potential to provide over one gigawatt of developable geothermal energy generation at present, with an additional 700 MWe over the next 12 years as the lake continues to recede. The field also has proven undeveloped reserves greater than double the current 392 MW$_e$ installed capacity that the field is currently generating from previously dry land.

A new conceptual model is now available that fits the observed field data and unique character of the field including its pork chop shape, one side of the field rising and the other side subsiding, the unexpected strike of the Brawley fault, stepping fault lines, chemistry changes, areas of distinct geologic disturbances, a unique pattern of rhyolite domes, successful and unsuccessful drilling in the field, and geophysical data.

This conceptual model can form the basis for continued exploration, development, and refinement of drilling targets, to provide even more prolific wells, as the SSGF becomes the largest geothermal field in the world.

Acknowledgements

We would like to thank Michael Angell of Neo Geologic for his review of the geologic structure aspects of the paper.

References

Brothers, D.S., Driscoll, N.W., Kent, G.M., Harding, A.J., Babcock, J.M., and Baskin, R.L., 2009. Tectonic Evolution of the Salton Sea Inferred from Seismic Reflection Data. Nature Geoscience 2, 581 – 584.

Burg, 1986, Strike-slip and oblique-slip tectonics. www.files.ethz.ch/structuralgeology/jpb/files/english/5wrench.pdf.

Elders, Wilfred, 1979. The Geological Background of the Geothermal Fields of the Salton Trough. Report # 79/24 for the Institute of Geophysics and Planetary Physics, pp. 20.

Elders, W.A. and Sass, J. H., 1988. The Salton Sea Scientific Drilling Project. Journal of Geophysical Research, Vol. 93 No. B11, 1988.

Elders, W., 1988, A Compendium of Reports on the Salton Sea Scientific Drilling Project.

Hulen, J., Kaspereit, D., Norton, D, Osborn, W., Pulka, F., 2002. Refined Conceptual Modeling and a New Resource Estimate for the Salton Sea Geothermal Field, Imperial Valley, California. Geothermal Resources Council Transactions, Vol. 26, pp.8.

Hulen, J., Norton, D., Kaspereit, D., Murray, L., Van de Putte, T., Wright, M., 2003. Geology and a Working Conceptual Model of the Obsidian Butte (Unit 6) Sector of the Salton Sea Geothermal Field, California. Geothermal Resources Council Transactions, Vol. 27.

Kaspereit, D., Berard, B., Gutierrez, P., Nichols, E., Jiuping, C., 2006. Land and Marine Magnetotelluric Exploration at the Salton Sea Geothermal Field. Geothermal Resources Council Transactions, 2006.

Lynch, D., Hudnut, K., Adams, P., 2013. Development of Recently Exposed Fumarole Fields near Mullet Island, Imperial County, California. Geomorphology, Vol. 195, pp 17.

Meidav, Tsvi; Howard, J.H., 1979. An Update of Tectonics and Geothermal Resource Magnitude of the Salton Sea Geothermal Resource. Geothermal Resources Council Transactions, Vol. 3 pp.5.

Newmark, R. L., P. W. Kasameyer, and L. W. Younker, 1988. Shallow Drilling in the Salton Sea Region: The Thermal Anomaly. J. Geophys. Res., Vol. 93 pp.18.

Nichols, Edward, Schlumberger, 2009. Final Report: Geothermal Exploration Under the Salton Sea Using Marine Magnetotellurics. Prepared for California Energy Commission, pp. 95.

Salton Sea Scientific Drilling Project: A Summary of Drilling and Engineering Activities and Scientific Results, Final Report, 1992. DOE/CE-12429-H1.

Shearer et al., 2005. Historical Map of the Brawley Seismic Zone 1981-2005. www.cisn.org.